Melatonin Reduces Angiogenesis in Serous Papillary Ovarian Carcinoma of Ethanol-Preferring Rats

Yohan Ricci Zonta [1], Marcelo Martinez [2], Isabel Cristina Cherici Camargo [3], Raquel Fantin Domeniconi [1], Luiz Antonio Lupi Júnior [1], Patricia Fernanda Felipe Pinheiro [1], Russel J. Reiter [4], Francisco Eduardo Martinez [1] and Luiz Gustavo De Almeida Chuffa [1,*]

[1] Department of Anatomy, São Paulo State University (Unesp), Institute of Biosciences, Botucatu-SP 18618-970, Brazil; yohanzonta@hotmail.com (Y.R.Z.); rdomeniconi@ibb.unesp.br (R.F.D.); lupijr@ibb.unesp.br (L.A.L.J.); pinheiro@ibb.unesp.br (P.F.F.P.); martinez@ibb.unesp.br (F.E.M.)

[2] Department of Morphology and Pathology, UFSCar—Universidade Federal de São Carlos, São Carlos-SP 13565-905, Brazil; martinez@ufscar.br,

[3] Department of Biotechnology, School of Sciences, Humanities and Languages, São Paulo State University (Unesp), Assis-SP 19806-900, Brazil; camargo@assis.unesp.br

[4] Department of Cellular and Structural Biology, UTHSCSA, San Antonio, TX 78229, USA; reiter@uthscsa.edu

Running title: Melatonin modulates angiogenesis in ovarian cancer

***Corresponding author:**

Luiz Gustavo de Almeida Chuffa, Department of Anatomy, Institute of Biosciences, UNESP – São Paulo State University, Zip Code: 510; P.O Box: 18618-970, Rubião Júnior, s/n, Botucatu, SP – Brazil, Phone: +55 (14) 3880-0027, Fax: +55 (14) 3811-6361. E-mail: chuffa@ibb.unesp.br

Peer-reviewed version available at Int. J. Mol. Sci. 2017, 18, , 763; doi:10.3390/ijms18040763

Abstract

Angiogenesis is a hallmark of ovarian cancer (OC) it promotes rapid cell growth and the associated metastasis. Identifying new bioactive compounds to target angiogenesis may provide valuable paradigms as therapeutic strategies. Melatonin is a well-characterized indoleamine that possesses important anti-angiogenic properties in a set of aggressive solid tumors. Herein, we evaluated the role of melatonin therapy on the angiogenic signaling pathway in OC of an ethanol-preferring rat model that mimics the same pathophysiological conditions occurring in women. OC was chemically induced with a single injection of 7,12-dimethylbenz(a)anthracene (DMBA) under the ovarian bursa. After the rats developed serous papillary OC, half of the animals received i.p. injections of melatonin (200 µg/100 g body weight/day) for 60 days. Serum levels of melatonin were higher following therapy, and the expression of its receptor MT1R was significantly increased in OC-bearing rats, regardless of ethanol intake. TGFB1, a transforming growth factor-beta1, was reduced only after melatonin treatment. Importantly, vascular endothelial growth factor (VEGF) was severely reduced after melatonin therapy in animals given or not given ethanol. Conversely, the levels of VEGF receptor 1 (VEGFR1) was diminished after ethanol consumption, regardless of melatonin therapy, and VEGFR2 was only reduced following melatonin. Hypoxia-inducible factor (HIF)-1α was augmented with ethanol consumption, and notably, melatonin significantly reduced their levels. Collectively, our results suggest that melatonin attenuates angiogenesis in OC of an animal model of ethanol consumption; this provides a possible complementary therapeutic opportunity for concurrent OC chemotherapy.

Keywords: ovarian cancer; melatonin; angiogenesis; VEGF; VEGFR; HIF-1α

1. Introduction

Ovarian cancer (OC) is the most lethal gynecological carcinoma among women and it exhibits poor prognosis when diagnosed in an advanced stage (< 50 % with a survival rate at 5 years) [1]. Even with the current therapies, including chemotherapy and surgical removal, patients in stage III or IV experience only a 20% survival rate [2, 3]. To date, early-stage OC has no apparent symptoms, and no significant screening method is yet available [4].

The influence of chronic alcoholism in the acquisition and progression of many types of cancer is indisputable. Alcohol abuse is associated with several changes in the reproductive system, such as including alterations of menopause, anovulation, infertility and even cancer [5, 6]. Moreover, acetaldehyde originating from ethanol oxidation acts as a co-carcinogenic agent through association with DNA, and by promoting cross-links between pairs of bases G:A and A:T [7, 8]. Notably, we have developed a useful ethanol-preferring rat model that strictly reflects the aspects of serous papillary OC after chemical induction with a carcinogen [9, 10]; this model provides an appropriate histological and molecular background that is needed to evaluate new chemoprotective compounds.

Angiogenesis is a complex and determining event for tumor growth and metastatic spread [11]. Its dynamic evolution is dependent on pro- and anti-angiogenic molecules. Vascular endothelial growth factor (VEGF) is highly expressed in tumor cells under numerous conditions such as hypoxia, acidosis, mechanical stress, and an imbalance of tumor suppressor genes. The VEGF receptor (VEGFR) is expressed on the surface of OC cells, and is associated with the development of malignant ascites and tumor progression [12]. Expressions of VEGFR1 and VEGFR2 are significantly elevated in OC cells, and specifically, the VEGFR2 is more functionally active in

decreasing microvascular density [13]. The synthesis of VEGF and its receptors is regulated by the hypoxia-inducible factor 1-alpha (HIF-1α), a heterodimer sensitive to the fluctuations in oxygen levels [14]. Under hypoxia, HIF-1α is stabilized and enters the nucleus where it binds to the hypoxia responsive elements (HRE) to activate the transcription of many genes related to tumor aggressiveness and chemoresistance [15, 16]. While VEGF targeted therapies (e.g. bevacizumab - a monoclonal humanized antibody against VEGF) showed positive results in clinical practice, its major effects are related to the optimal dose, duration of treatment, and specific OC subtype [17]. Importantly, the functional significance of VEGF/VEGFR signaling pathway is not completely understood in OC, and further studies are required. Recently, the transforming growth factor-β (TGF-β) was found to be associated with the occurrence, progression and metastasis of OC [18], and TGF-β production may represent an important strategy of tumor escape favoring angiogenesis and increasing the interaction between OC cells and components of the extracellular matrix [19].

Melatonin (*N*-acetyl-5-methoxytryptamine) is an indoleamine secreted in a circadian manner by the pineal gland with maximal production during the night [20]. It has remarkable functional versatility acting as antioxidant, immunomodulatory, and oncostatic agent in many cancer types including OC [4, 21-23]. At pharmacological concentrations, melatonin has anti-angiogenic activity [24, 25]. Recent publications have reported that melatonin significantly reduced the expression of VEGF and HIF-1α in breast and colon cancer in both in vitro and in vivo studies [26, 27], thus controlling neovascularization. To date, no study has elucidated the cross-talk between melatonin and angiogenesis in OC.

Herein, we investigated the influence of long-term melatonin therapy on the angiogenic process (VEGF/VEGFR/HIF-1α pathway) in serous papillary ovarian

Peer-reviewed version available at Int. J. Mol. Sci. 2017, 18, , 763; doi:10.3390/ijms18040763

carcinoma of an ethanol-preferring rat model. We further tested whether melatonin is effective in reducing angiogenesis in OC of animals exposed to ethanol.

2. Results

2.1. Anatomopathological analysis of OC and melatonin levels

The association between EtOH intake with DMBA led to high incidence of OC after 180 days of age. After treatments, the abdominal-pelvic cavity was opened and left ovary of the OC animals displayed solid masses with neovascularization spots differently from the ovaries of the OC+Mel group which exhibited soft and clear masses with no adhesions (Fig. 1A). Furthermore, histopathological analyses of the OC tissue confirmed the presence of serous papillary carcinoma with cellular atypia and exophytic architecture mixed with invasive gland-like neoplastic structures or tufts back-to-back (Fig. 1 B). Because the OC subtype was maintained, no microscopic changes were observed following EtOH consumption and melatonin therapy (Fig. 1 B I-IV). We further investigated the effects of melatonin on the OC masses, and notably, long-term melatonin significantly reduced the OC size by about 36% (Fig. 1 C). To validate the treatments, plasma melatonin was measured at the end of dark phase. The animals treated with melatonin (OC+Mel and OC+EtOH+Mel groups) showed higher levels of circulating melatonin than other groups (Fig. 1 D).

2.2. Melatonin therapy reduced the vessel density in OC

To confirm the effect of melatonin on tumor neovascularization, we performed a quantification of microvessel density (MVD) in seriated sections of OC tissue. The melatonin-treated animals showed a significant reduction of MVD compared to their controls, regardless of EtOH intake ($p<0.05$; Fig. 2 A, B).

2.3. MT1 is upregulated by melatonin in OC while TGF-β1 levels are downregulated

To investigate whether melatonin treatment alters the expression of its receptor, we measured MT1 intensity through immunofluorescence assays. MT1 was significantly increased by long-term melatonin therapy in epithelial cells of OC (Fig. 3 I and II; the fluorescence level was augmented from 37% ± 9.2 (OC group) to 86% ± 13.4 (OC+Mel group). Even in EtOH-drinking animals, melatonin therapy efficiently resulted in upregulation of MT1 (Fig. 3 III and IV; the fluorescence level increased from 32.8 ± 15.7 (OC+EtOH) to 79% ± 10.6 (OC+EtOH+Mel)). MT1 levels were further confirmed in serous papillary OC tissues, and immunoblots showed that melatonin therapy upregulated its own receptor MT1 in the OC+Mel (2.58-fold increased vs. OC; Table 1, Fig. 3 B and C) and OC+EtOH+Mel (2.34-fold increased vs. OC+EtOH; Table 1, Fig. 3 B and C) rats.

TGFβ1, an important factor associated with tumor migration and invasiveness, was only downregulated following melatonin therapy alone. In OC+Mel group, the epithelial cells of the papillae and stromal cells showed a weak signal for TGFβ1 (Table 1, Figs. 4 I and II), differently from the OC+EtOH+Mel group which showed a moderate signal (Table 1, Figs. 4 III and IV). Furthermore, the expression of TGFβ1 was significantly reduced after melatonin therapy (1.16-fold reduced vs. OC; Figs. 4 B and C).

2.4. Melatonin downregulates VEGF and VEGFR2 even in the presence of ethanol

We investigated the VEGF/VEGFR signaling pathway in OC tissues. Notably, VEGF was downregulated by melatonin in epithelial cells (1.40-fold reduction vs. OC; Table 1, Figs. 5 A I and II, B and C). Similarly, the combination of EtOH with melatonin promoted a significant reduction in the VEGF levels (2.19-fold reduction vs.

OC+EtOH; Table 1, Figs. 5 A III and IV, B and C). Unexpectedly, while VEGFR1 was unchanged by melatonin therapy ($p>0.05$; Fig. 5 A V and VI, B and C), their levels were downregulated by either EtOH alone or the combination of EtOH and melatonin (Table 1, Fig. 5 A VII and VIII, B and C), showing that EtOH consumption is responsible for VEGFR1 reduction. Conversely, melatonin therapy significantly reduced VEGFR2 levels in serous papillary OC, regardless of EtOH intake (Table 1, Fig. 5 A IX-XII). Also, melatonin alone (1.48-fold reduction vs. OC; Fig. 5 B and C), and the combination of EtOH and melatonin (1.77-fold reduction vs. OC+EtOH; Fig. 5 B and C) led to downregulation of VEGFR2.

2.5. HIF-1α is downregulated by melatonin only in the presence of EtOH intake

Although melatonin therapy seemed to slightly reduce HIF-1α immunostaining in the epithelial cells of OC+Mel and OC+EtOH+Mel groups (Table 1, Fig. 6 A I-IV), it was only significantly reduced in the OC+EtOH+Mel group (0.74-fold reduced vs. OC+EtOH; Fig. 6 B and C). EtOH consumption resulted in higher levels of HIF-1α compared to other groups and melatonin therapy efficiently restored these levels to near those in the OC rats.

2.6. Melatonin and ethanol differentially modulated the VEGF/VEGFR/HIF-1α pathway

Figure 7 summarizes the positive and negative regulatory effects which are influenced by either melatonin therapy or EtOH intake on angiogenic process in the serous papillary OC cell. In general, while EtOH upregulated VEGF and VEGFR2, treatment with melatonin efficiently suppressed the VEGF/VEGFR pathway resulting in reduced neovasculogenesis in OC. A part of this signaling response is thought to be mediated by the MT1 activation.

3. Discussion

Angiogenesis represents one of the hallmarks of tumor aggressiveness, and a number of anti-angiogenic agents have been tested in clinical trials, including in OC patients [28]. Although most investigations have demonstrated the prognostic value of VEGF in OC samples such as in surgical tissue, serum, and ascites, these results are somewhat inconsistent [29]. In an attempt to explore the effects of melatonin in an *in vivo* model of OC, we chemically induced OC in ethanol-preferring rats. This model has been shown to be appropriate for the development of aggressive OC subtypes similar to those occurring in women [9].

As uncovered in our previous studies [4, 30], melatonin treatment led to an increase of its circulating levels in both melatonin-treated groups, and was sufficient to reduce OC volume and mass, even in the presence of EtOH. The effects of melatonin on cell proliferation and apoptosis have been studied *in vitro*, basically using the serous papillary human OC cell line (SKOV-3) [31]. In pharmacological concentrations (0.5 - 2 mM), melatonin induced caspase-3 activation and cleavage of poly-(ADP-ribose) polymerase (PARP), resulting in the control of MAPK phosphorylation. In this regard, our previous work reported that long-term melatonin therapy downregulated survivin levels and upregulated p53, BAX, and active caspase-3, identifying a possible pathway by which melatonin promotes cell apoptosis in an in vivo model of OC [32].

We have observed that melatonin significantly reduced the levels of VEGF, VEGFR2, and HIF-1α regardless of EtOH consumption. In addition, melatonin alone lowered by half the levels of TGF-β1 compared to untreated OC-bearing rats. These effects seem to be mediated through its receptor MT1. Although no changes were observed in the histological aspects of the serous papillary OC, long-term melatonin treatment promoted anti-angiogenic activity to this tumor subtype as demonstrated by a

significant reduction in the microvessel density. Considering this function, melatonin could be a chemical strategy to limiting neovascularization in OC tissue.

Melatonin exerts antitumor effects through a variety of important mechanisms of action, making it difficult to determine which of these specific actions are most significant [33]. MT1 activation seems to be responsible for the oncostatic role of melatonin which results in inhibition of cAMP and related protein kinases [34, 35]. This regulatory activity can negatively alter the expression of genes involved in angiogenesis and migration pathways [36]. The expression of MT1 was higher in the surface of OC cell following melatonin therapy. Supporting this finding, treatment with exogenous nanomolar levels of melatonin upregulated MT1 expression in ovarian cancer SKOV-3 and OVCAR-3 cell lines [37], thus demonstrating a potential role of MT1 involvement in the regulation of downstream molecules related to angiogenic process.

TGF-β1 is overexpressed in cancer tissue, blood, and peritoneal fluid and it may contribute to OC progression and metastasis, in particular due to the regulation of the epithelial-to-mesenchymal transition [19]. Furthermore, TGF-β1 stimulates matrix metalloproteinase secretion thereby promoting OC cell invasion [38]. Several clinical studies report that TGF-β1 and TGF-β1-binding protein mRNAs are elevated in OC tissue and in ascites fluid [19, 39]. Although melatonin has been shown to activate the TGF-β1 pathway related to growth inhibition of breast cancer cells [40], we observed an antagonizing effect of melatonin on TGF-β1 and VEGF levels in the course of OC treatment. Together, these results indicated a favorable use of melatonin to protect against OC angiogenesis and metastasis.

A recent meta-analysis in woman with early and advanced stage OC found that both serum (385 patients) and tissue (638 patients) studies revealed a negative correlation between VEGF level and poor progression-free survival or overall survival

[29]. In epithelial OC, VEGF is involved in tumor progression and lymphatic metastasis, and VEGFR is aberrantly activated in OC subsets [41, 42]. After VEGFR activation, cancer stem cells undergo differentiation which in turn enhances survival, proliferation, migration, and invasion [43]. Herein, melatonin efficiently attenuated VEGF at the protein level. Strengthening this finding, other studies documented that higher concentrations of melatonin reduce the levels of VEGF mRNA and protein in human pancreatic carcinoma cells, prostate, colon, and breast cancer cells [26, 44-46]. Conversely, VEGFR1 was profoundly reduced in EtOH-consuming animals with or without melatonin treatment. In particular, VEGFR1 was only downregulated after EtOH intake. Reinforcing these data, it has been shown that EtOH disrupts VEGFR expression and activation of endothelial cells in reproductive tissues [47]. Although alcohol has many adverse effects in tumor development and progression, chronic EtOH consumption was associated to a reduced angiogenic signaling by lowering VEGFR1 levels in OC tissue. Melatonin therapy significantly downregulated VEGFR2, regardless of EtOH intake. VEGFR2 is the isoform predominantly expressed in malignant OC tissue [48], and treatment with anti-VEGFR2 drugs decreased OC cell migration and invasion [49].

The VEGF/VEGFR2 signaling between endothelial cells and tumor cells is one of the most representative systems for tumor-associated angiogenesis [50]; long-term melatonin therapy significantly attenuated this signaling in OC, possibly indicating a dual function of melatonin in inhibiting paracrine pathways created between tumor cells and the vessel endothelium. Consistent with our results, a recent study demonstrated that melatonin reduced the expression of VEGFR2 in breast cancer cells (MCF-7 and MDA-MB-231 cell lines), and also in mammary tumors of athymic nude mice [27, 51].

Angiogenesis occurs in response to conditions of low nutrients and oxygen levels, as modulated by HIF-1α [52]. This process is complex and highly dependent on pro- and anti-angiogenic factors. In fact, HIF-1α is critical for the regulation of VEGF gene transcription [53], although VEGF can be controlled by some oncogenes and growth factors. In our study, we found that melatonin did not alter the levels of activated HIF-1α in OC tissue, thus revealing a distinct response in reducing VEGF levels different from a transcriptional regulation by HIF-1α. These data provide clues for understanding new mechanisms related to melatonin-mediated inhibition of angiogenesis in OC, and might aid in uncovering novel combination therapies to control tumor growth. Recently, a number of mechanisms underlying melatonin's effects on the levels of HIF-1α and VEGF have been discussed, such as via its antioxidant capacity [23, 54], functional alteration of the ubiquitin ligase, von Hippel-Lindau (VHL) protein [55], changes in particular microRNA, and others [56]. While some hypotheses have been provided, the mechanisms regulating shifts in the balance of angiogenic activators and regulators remain inconclusive for OC.

The current results support an interesting relationship involving VEGF, VEGFRs, and HIF-1α in OC cell. In this context, melatonin differentially modulated this angiogenic pathway, contributing to a slow growing of the tumors. In addition, melatonin has been proven to significantly reduce OC size and microvessel density which may adversely impact tissue perfusion, and subsequently, the tumor development. Besides acting on tumor cells, melatonin also exhibits a direct anti-angiogenic activity by inhibiting the proliferation and migration of endothelial cells, as observed here as indicated by low microvessel density. Through its effects, we hypothesized that melatonin could serve as an effective agent for hypoxic adaptation and inhibition of angiogenesis in aggressive tumors (e.g. ovarian tumor), providing a

solid foundation for the use of melatonin in basic and preclinical studies. Furthermore, administration of melatonin is well tolerated, causing no local or systemic toxicity even after longer period of treatment.

4. Materials and Methods

4.1. Animals

Sixty UChB rats (a model of ethanol-preferring rat that has been developed by selective inbreeding), 65-day-old, weighing approximately 200 g, were obtained from the Department of Anatomy, Institute of Biosciences/Campus of Botucatu, UNESP – São Paulo State University. All animals were individually housed in polypropylene cages (43 x 30 x 15 cm) with autoclaved pine shavings as substrate, and maintained under constant room temperature (23±1ºC) and lighting conditions (12-h light/dark cycle, with the lights switched on at 06:00 h). The animals were provided with solid diet consisting of Nuvital® rodent chow and filtered water *ad libitum*.

4.2. Experimental design

Initially, the animals were divided into two groups (n=30): EtOH group, in which the rats had free access to a 10% (v/v) ethanol solution or water *ad libitum*, and a control group, which was composed of ethanol-naïve rats without access to ethanol. When the animals reached 65 days of age, they were given a choice between two bottles containing either water or a 10% (v/v) ethanol solution *ad libitum* over a period of 15 days. The animals displaying EtOH consumption ranging from 2-3 g of EtOH/kg/day were selected according to the procedure described by Chuffa et al. [57, 58].

When the rats were 80 days old, they were chemically induced with the carcinogen 7,12-dimethylbenz(a)anthracene (DMBA; Sigma Chemical Co, St Louis,

MO), via single injection into the ovarian bursa. During the next 120 days the rats were monitored for OC development by ultrasonography, and ovaries size was used as a representative parameter. After OC development (260-days-old), half of the animals received melatonin (M-5250, Sigma-Aldrich, St. Louis, MO, USA) intraperitoneally at dose of 200 µg/100 g body weight dissolved in 0.04 mL of 95% EtOH, and then diluted in 0.3 mL of 0.9% NaCl (vehicle) at a steady-state concentration of 0.3 mg/mL. The daily injections were administered at night (19 – 19:30 h) over the period of 60 days [59].

Finally, the animals were divided into four groups (n = 15): OC group: DMBA-induced animals that did not consume EtOH; OC+Mel group: DMBA-induced animals that received melatonin as therapy; OC+EtOH group: DMBA-induced animals that consumed 10% EtOH solution during OC development; and OC+EtOH+Mel group: DMBA-induced animals that consumed 10% EtOH solution during OC development and received melatonin as therapy. After all procedures, the animals were carefully anesthetized and euthanized during early morning for OC tissue and blood collection. The present experimental protocol was accepted by the Ethical Committee of the Institute of Bioscience/UNESP (CEEA).

4.3. Intraovarian injection of DMBA for tumor initiation

After selection for voluntary ethanol consumption, the animals (n = 60) were anesthetized with ketamine hydrochloride (60 mg/kg, i.p.) and xylazine (5 mg/kg, i.p.), and a 2-cm incision was made through the skin and muscles for accessing the left ovaries. The left ovarian bursa was identified and the space filled with a single injection of 100 µg DMBA (Sigma Chemical Co, St Louis, MO) diluted in 10 µL sesame oil, used as the vehicle [60]. After moving the ovaries back to the cavity, the muscle layer

and skin was closed using a 3-0 silk suture. Concomitantly, the right ovary underwent sham-surgery (control ovary) using only the vehicle. All animals received prophylactic treatment with antibiotic (10^5 units of benzylpenicillin potassium via i.p.). Over the next days, OC development was observed by ultrasonography.

4.4. Melatonin levels

After plasma collection, melatonin was extracted (n = 15 samples/group) using HPLC-grade methanol followed by separation on columns (Sep-Pak Vac C-18, reverse phase, 12.5 nm; Water Corporation, Milford, Massachusetts, USA). 50 µL of samples were used and assayed in a Coat-a-count Melatonin ELISA Kit and read at 405 nm. The samples were run in duplicate and the coefficient of variation was 4%. All reagents and microtiter plates were purchased from IBL (IBL International, Hamburg, Germany), and the concentrations were given as the pg/mL.

4.5. Histopathology

Following euthanasia, the ovaries (n=7) were individually collected and immediately fixed in 10% (v/v) buffered formalin for 24h. After fixation, OC tissues were washed and dehydrated in graded ethanol, diaphanized in xylene and embedded in paraplastic (Oxford Labware, St. Louis, USA). 5-µm-thick sections were made using a Leica RM 2165 microtome and every 20th section was stained with hematoxylin and eosin (H&E). Histopathological evaluation was carried out by a pathologist with expertise in animal malignancies and only serous papillary carcinoma was considered for further analysis.

4.6. Vascular density

The micro-vessel density (MVD) was detected by H&E staining. Five random "hot spots" with high concentration of vessels were identified in each slides (n=7 animals/group) and positive areas were counted in a double fashion condition. Total histological area (mm^2) was considered, and MVD was calculated as previously reported [61].

4.7. Immunofluorescence

OC tissues were washed in PBS, sodium chloride, potassium chloride, dihydrogen phosphate, and disodium hydrogen phosphate), followed by fixation in 4% paraformaldehyde for 10 min, and permeabilization with PBS. After blocking nonspecific binding sites with 1% bovine serum albumin (BSA), samples were incubated with anti-MT1 primary rabbit polyclonal antibody (dilution 1:100, overnight at 4º C) followed by secondary polyclonal anti-rabbit IgG conjugated to FITC (1:250, sc-2012, Santa Cruz Biotechnology Inc., CA, USA) for 1 h. DAP1 was used for nuclei staining (5 min) at room temperature. For negative immunolabeling, the primary antibody was omitted. Immunopositive reactions were analyzed using a fluorescence microscope (Zeiss Axiophot II, Oberkochen, Germany) at 40X magnification (emission filter at 650 nm for FITC and emission filter at 485 nm for DAPI staining). The fluorescence analysis in merged images was performed using the Image J software.

4.8. Immunohistochemistry

For immunohistochemistry, sections of OC (n = 7/group) were deparaffinized based on the areas previously identified during the histopathology analysis. Antigen retrieval was performed in a microwave for 15 min (3 X 5 min) using 0.01 M sodium

citrate buffer, pH 6.0. After endogenous peroxidase was blocked, the tissues were incubated with 3% BSA for 1 h. Then, OC sections were incubated overnight with primary antibodies (Abcam, Cambridge, UK: TGFβ1, VEGF, VEGFR1, VEGFR2, HIF-1α) at dilution 1:100. After immunoreactions, sections were washed in TBS-T buffer and incubated with polymer Anti-Mouse IgG or Anti-Rabbit - DAKO ® CYT) for 1h. The slides were reacted with diaminobenzidine (DAB; Sigma, St. Louis, MO, USA) for 5 min, and sections were finally counterstained with hematoxylin. Negative controls were obtained by omitting the primary antibody. IHC analyses were performed under a Zeiss Axiophot II microscope (Carl Zeiss, Oberkochen, Germany) based on the levels of staining intensity (absent 0, weak +, moderate ++ and strong +++).

4.9. Western blot

100 mg of OC samples (n=7) were rapidly frozen in liquid nitrogen and stored at - 80ºC. Only OC tissues containing serous papillary tumors were homogenized with RIPA lysis buffer (Pierce Biotechnology, Rockford, IL, USA) supplemented with protease inhibitors. The homogenates were centrifuged at 21,912 g for 20 min at 4ºC to remove cell debris, and total protein was measured through Bradford colorimetric method. After 70 µg protein was added to 1.5 X Laemmli buffer, individual samples were loaded per well and resolved into 4-12% acrylamide gradient gels (Amersham Biosciences, Uppsala, Sweden) for 2h at 60 mA. After electrophoresis, proteins were electrotransferred to nitrocellulose membranes for 1.5 h at 200 mA. Prestained standards (Bio-Rad, Hercules, CA, USA) were used as molecular weight markers. Then, the membranes were blocked with TBS-T solution containing 3% BSA for 60 min followed by incubation with the following antibodies: anti-TGFβ1, anti-VEGF, anti-VEGFR1, anti-VEGFR2, anti-HIF-1α (Abcam, Cambridge, UK; 1:1000 dilutions in 1% BSA). The membrane was washed in basal solution (1% TBS-T) and incubated with

Peer-reviewed version available at *Int. J. Mol. Sci.* **2017**, *18*, , 763; doi:10.3390/ijms18040763

secondary antibody conjugated with HRP (1:10000 dilution; Sigma, St. Louis, MO, USA) for 1 h. Thereafter, blot signals were developed using an ECL detection kit (Thermo Scientific). Bands were obtained from individual blots of 7 animals/group using image J analysis software. B-actin was used as positive control, and data were expressed as the mean ± SD. Immunoblotting were represented as optical densitometry index (% band intensity).

4.10. Statistical analysis

All data are presented as the mean ± SD, and analyses were performed using one-way ANOVA. Significant results were subjected to *post-hoc* Tukey test, and statistical significance was set at $P < 0.05$. The GraphPad Prism 5.0 (La Jolla, CA, USA) software was used.

5. Conclusions

In summary, the present study investigated the cross-talk between the VEGF/VEGFR/HIF-1α system and melatonin therapy in an ethanol-preferring rat model of ovarian carcinoma. Melatonin significantly reduced OC mass and microvessel density, thus limiting the potential aggressiveness of serous papillary OC. Furthermore, melatonin therapy exerted anti-angiogenic effects by reducing angiogenic factors (TGFβ1, VEGF, and VEGFR2) related to malignancies in OC, regardless of ethanol consumption. In ethanol-drinking animals, the high levels of HIF-1α were significantly reduced following melatonin therapy. Overall, our findings indicate that melatonin's regulatory signaling is mediated via its receptor MT1, suggesting melatonin as an adjuvant strategy against angiogenesis in OC.

Disclosure statement

The authors have nothing to disclose.

Author contributions

LGAC, FEM, YRZ, LALJ: collected and analyzed the data, drafted the manuscript, and conceived the main idea of the study. MM, ICCC, PFFP, RFD: participated in the acquisition of data and in the design and intellectual conception of the study. RJR: analyzed and critically reviewed the paper. All authors performed the statistical analysis and approved the final version of the manuscript.

Acknowledgments

We are grateful to Mr Thiago da Silva and Mr. Gelson Rodriguez from Department of Anatomy, IBB/UNESP, Botucatu-SP, for excellent technical support.

Financial support

We would like to give a special thanks to FAPESP (Fundação de Amparo à Pesquisa do Estado de São Paulo, Process number: 2016/03993-9, 2015/16315-6, 2013/02466-7) and Prointer (Prope/UNESP) by providing financial support.

References

1. Siegel, R.L.; Miller, K.D.; Jemal, A. Cancer Statistics, 2016. *CA Cancer J Clin.* **2016**, *66*, 7-30.

2. Armstrong, D.K.; Bundy, B.; Wenzel, L.; Huang, H.Q.; Baergen, R.; Lele, S.; Copeland, L.J.; Walker, J.L.; Burger, R.A. Intraperitoneal cisplatin and paclitaxel in ovarian cancer. *N Engl J Med.* **2006**, *354*, 34-43.

3. Kurman, R.J.; Shih, I.M. Pathogenesis of ovarian cancer. Lessons from morphology and molecular biology and their clinical implications. *Int J Gynecol Pathol*. **2008**, *27*, 151-160.

4. Chuffa, L.G.; Fioruci-Fontanelli, B.A.; Mendes, L.O.; Ferreira Seiva, F.R.; Martinez, M.; Fávaro, W.J.; Domeniconi, R.F.; Pinheiro, P.F.; Delazari Dos Santos, L.; Martinez, F.E. Melatonin attenuates the TLR4-mediated inflammatory response through MyD88- and TRIF-dependent signaling pathways in an in vivo model of ovarian cancer. *BMC Cancer*. **2015**, *15*, 34.

5. Carrara, O.; Oger-Jeannin, V.; Desechalliers, J.P. Disorders of the hypothalamo-hypophyseal-ovarian axis in chronic alcoholic women. *Rev Med Interne.* **1993**, *14*, 9-13.

6. Henderson, J.; Gray, R.; Brocklehurst, P. Systematic review of effects of low-moderate prenatal alcohol exposure on pregnancy outcome. *BJOG.* **2007**, *114*, 243-252.

7. Seitz, H.K.; Stickel, F. Molecular mechanisms of alcohol-mediated carcinogenesis. *Nat Rev Cancer.* **2007**, *7*, 599-612.

8. Berstad, P.; Ma, H.; Bernstein, L.; Ursin, G. Alcohol intake and breast cancer risk among young women. *Breast Cancer Res Treat.* **2008**, *108*, 113-120.

9. Chuffa, L.G.; Fioruci-Fontanelli, B.A.; Mendes, L.O.; Fávaro, W.J.; Pinheiro, P.F.; Martinez, M.; Martinez, F.E. Characterization of chemically induced ovarian carcinomas in an ethanol-preferring rat model: influence of long-term melatonin treatment. *Plos One.* **2013**, *8*, e81676.

10. Chuffa, L.G.; Lupi Júnior, L.A.; Seiva, F.R.; Martinez, M.; Domeniconi, R.F.; Pinheiro, P.F.; Dos Santos, L.D.; Martinez, F.E. Quantitative proteomic profiling reveals that diverse metabolic pathways are influenced by melatonin in an in vivo model of ovarian carcinoma. *J Proteome Res.* **2016,** *15*, 3872-3882.

11. Dvorak, H.F. Vascular permeability factor/vascular endothelial growth factor: a critical cytokine in tumor angiogenesis and a potential target for diagnosis and therapy. *J Clin Oncol.* **2002**, *20*, 4368–4380.

12. Duncan, T.J.; Al-Attar, A.; Rolland, P.; Scott, I.V.; Deen, S.; Liu, D.T.; Spendlove, I.; Durrant, L.G. Vascular endothelial growth factor expression in ovarian cancer: a model for targeted use of novel therapies? *Clin Cancer Res.* **2008**, *14*, 3030-3035.

13. Wang, E.S.; Teruya-Feldstein, J.; Wu, Y.; Zhu, Z.; Hicklin, D.J.; Moore, M.A. Targeting autocrine and paracrine VEGF receptor pathways inhibits human lymphoma xenografts in vivo. *Blood.* **2004**, *104*, 2893-2902.

14. Germain, S.; Monnot, C.; Muller, L.; Eichmann, A. Hypoxia-driven angiogenesis: role of tip cells and extracellular matrix scaffolding. *Curr Opin Hematol.* **2010**, *17*, 245-251.

15. Maxwell, P.H.; Pugh, C.W.; Ratcliffe, P.J. Activation of the HIF pathway in cancer. *Curr Opin Genet.* **2001**, *11*, 293–299.

16. Vaupel, P.; Mayer, A. Hypoxia in cancer: significance and impact on clinical outcome. *Cancer Metastasis Rev*. **2007**, *26*, 225-239.

17. Reinthaller, A. Antiangiogenic therapies in ovarian cancer. *Memo.* **2016**, *9*, 139-143.

18. Wang, S-T.; Liu, J.J.; Wang, C.Z.; Lin, B.; Hao, Y.Y.; Wang, Y.F.; Gao, S.; Qi, Y.; Zhang, S.L.; Iwamori, M. Expression and correlation of Lewis y antigen and TGF-B1 in ovarian epithelial carcinoma. *Oncol Rep.* **2012**, *27*, 1065-1071.

19. Do, T.V.; Kubba, L.A.; Du, H.; Sturgis, C.D.; Woodruff, T.K. Transforming growth factor-beta1, transforming growth factor-beta2, and transforming growth factor-beta3 enhance ovarian cancer metastatic potential by inducing a Smad3-dependent epithelial-to-mesenchymal transition. *Mol Cancer Res*. **2008**, *6*, 695-705.

20. Stehle, J.H.; Saade, A.; Rawashdeh, O.; Ackermann, K.; Jilg, A.; Sebestény, T.; Maronde, E. A survey of molecular details in the human pineal gland in the light of phylogeny, structure, function and chronobiological diseases. *J Pineal Res.* **2011**, *51*, 17-43.

21. Reiter, R.J. Mechanisms of cancer inhibition by melatonin. *J Pineal Res.* **2004**, *3*, 213-214.

22. Reiter, R.J.; Tan, D.X.; Galano, A. Melatonin: exceeding expectations. *Physiology* (Bethesda). **2014**, *29*, 325-333.

23. Reiter, R.J.; Mayo, J.C.; Tan, D.X.; Sainz, R.M.; Alatorre-Jimenez, M.; Qin, L. Melatonin as an antioxidant: under promises but over delivers. *J Pineal Res* **2016**, *61*, 253-278.

24. Carbajo-Pescador, S.; Ordoñez, R.; Benet, M.; Jover, R.; García-Palomo, A.; Mauriz, J.L.; González-Gallego, J. Inhibition of VEGF expression through blockade of Hif1α and STAT3 signalling mediates the anti-angiogenic effect of melatonin in HepG2 liver cancer cells. *Br J Cancer.* **2013**, *109*, 83-91.

25. Zhang, T.; Wu, X.; Ke, C.; Yin, M.; Li, Z.; Fan, L.; Zhang, W.; Zhang, H.; Zhao, F.; Zhou, X.; et al. Identification of potential biomarkers for ovarian cancer by urinary metabolomic profiling. *J Proteome Res.* **2013**, *12*, 505-512.

26. Park S.Y.; Jang, W.J.; Yi, E.Y.; Jang, J.Y.; Jung, Y.; Jeong, J.W.; Kim, Y.J. Melatonin suppresses tumor angiogenesis by inhibiting HIF-1 alpha stabilization under hypoxia. *J Pineal Res.* **2010**, *48*, 178-184.

27. Jardim-Perassi, B.V.; Arbab, A.S.; Ferreira, L.C.; Borin, T.F.; Varma, N.R.; Iskander, A.S.; Shankar, A.; Ali, M.M.; de Campos Zuccari, D.A. Effect of melatonin on tumor growth and angiogenesis in xenograft model of breast cancer. *PLoS One.* **2014**, *9*, e85311.

28. Burger, R.A. Antiangiogenic agents should be integrated into the standard treatment for patients with ovarian cancer. *Ann Oncol*. **2011**, *22*, viii65-viii68.

29. Yu, L.; Deng, L.; Li, J.; Zhang, Y.; Hu, L. The prognostic value of vascular endothelial growth factor in ovarian cancer: A systematic review and meta-analysis. *Gynecol Oncol.* **2013**, *128*, 391-396.

30. Ferreira, G.M.; Martinez, M.; Camargo, I.C.; Domeniconi, R.F.; Martinez, F.E.; Chuffa, L.G. Melatonin attenuates Her-2, p38 MAPK, p-AKT, and mTOR levels in ovarian carcinoma of ethanol-preferring rats. *J Cancer.* **2014**, *5*, 728-735.

31. Kim, J.H.; Jeong, S.J.; Kim, B.; Yun, S.M.; Choi, D.Y.; Kim, S.H. Melatonin synergistically enhances cisplatin-induced apoptosis via the dephosphorylation of ERK/p90 ribosomal S6 kinase/heat shock protein 27 in SK-OV-3 cells. *J Pineal Res.* **2012**, *52*, 244-252.

32. Chuffa, L.G.; Alves, M.S.; Martinez, M.; Camargo, I.C.; Pinheiro, P.F.; Domeniconi, R.F.; Júnior, L.A.; Martinez, F.E. Apoptosis is triggered by melatonin in an in vivo model of ovarian carcinoma. *Endocr Relat Cancer.* **2016**, *23*, 65-76.

33. Di Bella, G.; Mascia, F.; Gualano, L.; Di Bella, L. Melatonin Anticancer Effects: Review. *Int J Mol Sci.* **2013**, *14,* 2410–2430.

34. Jablonska, K.; Pula, B.; Zemla, A.; Kobierzycki, C.; Kedzia, W.; Nowak-Markwitz, E.; Spaczynski, M.; Zabel, M.; Podhorska-Okolow, M.; Dziegiel, P. Expression of the MT1 melatonin receptor in ovarian cancer cells. *Int J Mol Sci.* **2014**, *15*, 23074-23089.

35. Hill, S.M.; Belancio, V.P.; Dauchy, R.T.; Xiang, S.; Brimer, S.; Mao, L.; Hauch, A.; Lundberg, P.W.; Summers, W.; Yuan, L.; Frasch, T.; Blask, D.E. Melatonin: an inhibitor of breast cancer. *Endocr Relat Cancer* **2015**, R183-R204.

36. Grant, S.G.; Melan, M.A.; Latimer, J.J.; Witt-Enderby, P.A. Melatonin and breast cancer: cellular mechanisms, clinical studies and future perspectives. *Expert Rev Mol Med.* **2009**, *11*, e5.

37. Treeck, O.; Haldar, C.; Ortmann, O. Antiestrogens modulate MT1 melatonin receptor expression in breast and ovarian cancer cell lines. *Oncol Rep.* **2006**, *15*, 231-235.

38. Lin, S.W.; Lee, M.T.; Ke, F.C.; Lee, P.P.; Huang, C.J.; Ip, M.M.; Chen, L.; Hwang, J.J. TGFβ1 stimulates the secretion of matrix metalloproteinase 2 (MMP2) and the invasive behavior in human ovarian cancer cells, which is suppressed by MMP inhibitor BB3103. *Clin Exp Metastasis.* **2000**, *18*, 493-499.

39. Santin, A.D.; Bellone, S.; Ravaggi, A.; Roman, J.; Smith, C.V.; Pecorelli, S.; Cannon, M.J.; Parham, G.P. Increased levels of interleukin-10 and transforming growth factor-β in the plasma and ascitic fluid of patients with advanced ovarian cancer. *BJOG.* **2001**, *108*, 804-808.

40. Proietti, S.; Cucina, A.; D'Anselmi, F.; Dinicola, S.; Pasqualato, A.; Lisi, E.; Bizzarri, M. Melatonin and vitamin D3 synergistically down-regulate Akt and MDM2 leading to TGFβ-1-dependent growth inhibition of breast cancer cells. *J Pineal Res.* **2011**, *50*, 150-158.

41. Becker, M.A.; Farzan, T.; Harrington, S.C.; Krempski, J.W.; Weroha, S.J.; Hou, X.; Kalli, K.R.; Wong, T.W.; Haluska, P. Dual HER/VEGF receptor targeting inhibits in vivo ovarian cancer tumor growth. *Mol Cancer Ther.* **2013**, *12*, 2909-2916.

42. He, L.; He, J.; Zhao, X. Expression of VEGF-D in epithelial ovarian cancer and its relationship to lymphatic metastasis. *Asia Pac J Clin Oncol.* **2016**, *12*, e161-166.

43. Ai, B.; Bie, Z.; Zhang, S.; Li, A. Paclitaxel targets VEGF-mediated angiogenesis in ovarian cancer treatment. *Am J Cancer Res.* **2016**, *6*, 1624-1635.

44. Dai, M.; Cui, P.; Yu, M.; Han, J.; Li, H.; Xiu, R. Melatonin modulates the expression of VEGF and HIF-1 alpha induced by CoCl2 in cultured cancer cells. *J Pineal Res.* **2008**, *44*, 121-126.

45. Park, J.W.; Hwang, M.S.; Suh, S.I.; Baek, W.K. Melatonin downregulates HIF-1 alpha expression through inhibition of protein translation in prostate cancer cells. *J Pineal Res.* **2009**, *46*, 415-421.

46. Alvarez-Garcia, V.; Gonzalez, A.; Alonso-Gonzalez, C.; Martinez- Campa, C.; Cos, S. Regulation of vascular endothelial growth factor by melatonin in human breast cancer cells. *J Pineal Res.* **2013**, *54*, 373-380.

47. Neves, D.R.; Tomada, I.M.; Assunção, M.M.; Marques, F.A.; Almeida, H.M.; Andrade, J.P. Effects of chronic red wine consumption on the expression of vascular endothelial growth factor, angiopoietin 1, angiopoietin 2, and its receptors in rat erectile tissue. *J Food Sci.* **2010**, *75*, H79-H86.

48. Nishida, N.; Yano, H.; Komai, K.; Nishida, T.; Kamura, T.; Kojiro, M. Vascular endothelial growth factor C and vascular endothelial growth factor receptor 2 are related closely to the prognosis of patients with ovarian carcinoma. *Cancer.* **2004**, *101*, 1364–74.

49. Spannuth, W.A.; Nick, A.M.; Jennings, N.B.; Armaiz-Pena, G.N.; Mangala, L.S.; Danes, C.G.; Lin, Y.G.; Merritt, W.M.; Thaker, P.H.; Kamat, A.A.; et al. Functional significance of VEGFR-2 on ovarian cancer cells. *Int J Cancer.* **2009,** *124*, 1045-1053.

50. Chatterjee, S.; Heukamp, L.C.; Siobal, M.; Schottle, J.; Wieczorek, C.; Peifer, M.; Frasca, D., Koker, M.; Konig, K.; Meder, L.; et al. Tumor VEGF:VEGFR2 autocrine feed-forward loop triggers angiogenesis in lung cancer. *J Clin Invest*. **2013**, *123*, 1732-1740.

51. Jardim-Perassi, B.V.; Lourenço, M.R.; Doho, G.M.; Grígolo, I.H.; Gelaleti, G.B.; Ferreira, L.C.; Borin, T.F.; Moschetta, M.G.; Pires de Campos Zuccari, D.A. Melatonin regulates angiogenic factors under hypoxia in breast cancer cell lines. *Anticancer Agents Med Chem.* **2016**, *16*, 347-358.

52. Milkiewicz, M.; Ispanovic, E.; Doyle, J.L.; Haas, T.L. Regulators of angiogenesis and strategies for their therapeutic manipulation. *Int J Biochem Cell Biol.* **2006**, *38*, 333–357.

53. Manalo, D.J.; Rowan, A.; Lavoie, T.; Natarajan, L.; Kelly, B.D.; Ye, S.Q.; Garcia, J.G.; Semenza, G.L. Transcriptional regulation of vascular endothelial cell responses to hypoxia by HIF-1. *Blood.* **2005**, *105*, 659–669.

54. Manchester, L.C.; Coto-Montes, A.; Boga, J.A.; Andersen, L.P.; Zhou, Z.; Galano, A.; Vriend, J.; Tan, D.X.; Reiter, R.J. Melatonin: an ancient molecule that makes oxygen metabolically tolerable. *J Pineal Res* **2015**, *59,* 403-419.

55. Vriend, J.; Reiter, R.J. Melatonin and the von Hippel-Lindau/HIF-1 oxygen sensing system: a review. *Biochim Biophys Acta* **2016**, *1865,* 176-183.

56. Su, S.C.; Hsieh, M.J.; Yang, W.E.; Chung, W.H.; Reiter, R.J.; Yang, S.F. Cancer metastasis: Mechanisms of inhibition by melatonin. *J Pineal Res.* **2017**, *62*, e12370.

57. Chuffa, L.G.; Seiva, F.R.; Fávaro, W.J.; Teixeira, G.R.; Amorim, J.P.; Mendes, L.O.; Fioruci, B.A.; Pinheiro, P.F.; Fernandes, A.A.; Franci, J.A.; et al. Melatonin reduces LH, 17 beta-estradiol and induces differential regulation of sex steroid receptors in reproductive tissues during rat ovulation. *Reprod Biol Endocrinol*. **2011**, *9*, 108.

58. Chuffa, L.G.; Seiva, F.R.; Fávaro, W.J.; Amorim, J.P.; Teixeira, G.R.; Mendes, L.O.; Fioruci-Fontanelli, B.A.; Pinheiro, P.F.; Martinez, M.; Martinez, F.E. Melatonin and ethanol intake exert opposite effects on circulating estradiol and progesterone and differentially regulate sex steroid receptors in the ovaries, oviducts, and uteri of adult rats. *Reprod Toxicol.* **2013**, *39*, 40-49.

59. Chuffa, L.G.; Amorim, J.P.; Teixeira, G.R.; Mendes, L.O.;, Fioruci, B.A.; Pinheiro, P.F.; Seiva, F.R.; Novelli, E.L.; Mello Júnior, W.; Martinez, M.; Martinez, F.E. Long-term melatonin treatment reduces ovarian mass and enhances tissue antioxidant defenses during ovulation in the rat. *Braz J Med Biol Res.* **2011**, *44*, 217-23.

60. Hoyer, P.B.; Davis, J.R.; Bedrnicek, J.B.; Marion, S.L.; Christian, P.J.; Barton, J.K.; Brewer, M.A. Ovarian neoplasm development by 7,12-dimethylbenz[a]anthracene (DMBA) in a chemically-induced rat model of ovarian failure. *Gynecol Oncol.* **2009**, *112*, 610-615.

61. Weidner, N.; Semple, J.P.; Welch, W.R.; Folkman, J. Tumor angiogenesis and metastasis-correlation in invasive breast carcinoma. *N Engl J Med.* **1991** *324*, 1–8.

Figure Legends

Figure 1. Development and treatment of OC. (A) Anatomopathological specimens of the untreated and melatonin-treated OCs. **(B)** Micrographs of the OCs showing serous papillary architecture in OC (I), OC+Mel (II), OC+EtOH (III), and OC+EtOH+Mel (IV) groups. Bar = 20 µm. **(C)** OC mass was measured at the end of treatments, ^{a} $P < 0.05$ vs. OC. **(D)** Plasma melatonin levels (pg/mL) after the last treatment dose, $^{a, b}$ $P < 0.05$ vs. OC and OC+EtOH, respectively. N=15 animals/group.

Peer-reviewed version available at Int. J. Mol. Sci. 2017, 18, , 763; doi:10.3390/ijms18040763

Figure 2. Analysis of the microvessel density. (A) Representative histological images showing the pattern of vascularization in OC (I), OC+Mel (II), OC+EtOH (III), and OC+EtOH+Mel (IV). Bar = 20 µm. **(B)** Quantitative analysis of micro-vessel density (%) was achieved by counting positive vessels in the field (white arrows). [a, b] $P < 0.05$ vs. OC and OC+EtOH, respectively. N=15 animals/group.

Figure 3. Immunofluorescence localization and western blot analysis of MT1 in serous papillary OC. (A) Merged images of the immunofluorescence of MT1 and DAPI nuclear staining in OC (I), OC+Mel (II), OC+EtOH (III) and OC+EtOH+Mel (IV) groups; (Alexa fluor® 488, Bar = 20 µm, negative controls were used). **(B)** Representative MT1 profile of extracts (70 µg proteins) pooled from 7 samples/group (left panel). **(C)** Extracts obtained from individual animals were used for densitometric analysis of the MT1 levels following normalization to the β-actin. Data are expressed as the mean ± SD (n = 7). [a] $P < 0.05$ vs. OC; [b] $P < 0.05$ vs. OC+EtOH.

Figure 4. Immunohistochemical localization and western blot analysis of TGFβ1 in serous papillary OC. (A) The immunoreaction of TGFβ1 in the epithelial cells of OC was stronger in the OC **(I)** and OC+EtOH **(III)** groups compared to a weak reaction observed in OC+Mel **(II)** and OC+EtOH+Mel **(IV)** animals (black arrows). Bar = 20 µm. Negative controls were used. **(B)** Representative TGFβ1 profile of extracts (70 µg proteins) pooled from 7 samples/group (left panel). **(C)** Extracts obtained from individual animals were used for densitometric analysis of the proteins following normalization to house-keeping protein β-actin. All results are expressed as the mean ± SD (n = 7). [a] $P < 0.05$ vs. OC.

Figure 5. Immunohistochemical localization and western blot analysis of VEGF, VEGFR1, and VEGFR2 in serous papillary OC. (A) The immunoreaction of VEGF was moderate to high in the OC **(I)** and OC+EtOH **(III)** groups while the groups OC+Mel **(II)** and OC+EtOH+Mel **(IV)** showed a weak reaction after melatonin treatment (black arrow). The immunoreactions of VEGFR1 varied from weak to moderate in the surface epithelium of the OC **(V)** and OC+Mel **(VI)** animals, and only a weak reaction was notable in the OC+EtOH **(VII)** and OC+EtOH+Mel **(VIII)** groups (black arrow). A strong reaction to VEGFR2 was present in the papillae epithelium of the OC **(IX)** and OC+EtOH **(XI)** groups, and melatonin treatment led to weak or even absence of VEGFR2 immunostaining in the OC+Mel **(X)** and OC+EtOH+Mel **(XII)** animals (black arrows). Bar = 20 µm. Negative controls were used. **(B)** Representative profile of the VEGF, VEGFR1, and VEGFR2 levels obtained from protein extracts (70 µg) pooled from 7 samples/group (upper panel). **(C)** Extracts obtained from individual animals were used for densitometric analysis of the proteins following normalization to house-keeping protein (β-actin). Data are expressed as the mean ± SD (n = 7). ^{a} $P < 0.05$ vs. OC; ^{b} $P < 0.05$ vs. OC+Mel; ^{c} $P < 0.05$ vs. OC+EtOH.

Figure 6. Immunohistochemical localization and western blot analysis of HIF-1α in serous papillary OC. (A) The immunoreaction of HIF-1α in the epithelial cells of OCs was moderate to weak in the OC **(I)** and OC+Mel **(II)** groups compared to a strong reaction observed in OC+EtOH **(III)** animals. In OC+EtOH animals, melatonin treatment reduced the HIF-1α intensity closely to control levels **(IV)** (black arrows). Bar = 20 µm. Negative controls were used. **(B)** Representative HIF-1α profile of extracts (70 µg protein) pooled from 7 samples/group (left panel). **(C)** Extracts obtained from individual animals were used for densitometric analysis of the proteins following

normalization to house-keeping protein β-actin. Data are expressed as the mean ± SD (n = 7). [a] $P < 0.05$ vs. OC; [b] $P < 0.05$ vs. OC+Mel; [d] $P < 0.05$ vs. OC+EtOH+Mel.

Figure 7. Schematic representation of the VEGF/VEGFR/HIF-1α signaling pathway and the effects of melatonin treatment leading to the activation or repression of downstream molecules in OC cell. This activation seems to be mediated by MT1 and possibly via clock genes. Intracellular signaling results in the phosphorylation cascade and, under normoxia, HIF-1α is degraded via the proteasome pathway. Otherwise, under hypoxia condition, the stabilized HIF-1α is translocated to the nucleus to promote the transactivation of target genes related to tumor progression/differentiation, angiogenesis, and vasomotion. VEGF, VEGFR2, HIF-1α, and TGFβ1 are downregulated by Mel and/or the association EtOH+Mel. Melatonin therapy also positively regulated MT1 expression in OC.

Table 1. Analysis of the immunohistochemical and fluorescence staining.

Target proteins	*Treatments*			
	OC	OC+Mel	OC+EtOH	OC+EtOH+Mel
MT1	+	++	+	++
TGFβ1	+++	+	+++	++
VEGF	++	+	+++	+
VEGFR1	+/++	+/++	+	0/+
VEGFR2	+++	+	+++	0/+
HIF-1α	++	+	++/+++	+

Visual OC scoring was evaluated by a pathologist. Representative score was as 0 (no signal), + (weak signal), ++ (moderate signal), or +++ (strong signal). N = 10 animals/group. Five OC sections per animal were randomly chosen.

Figure 1

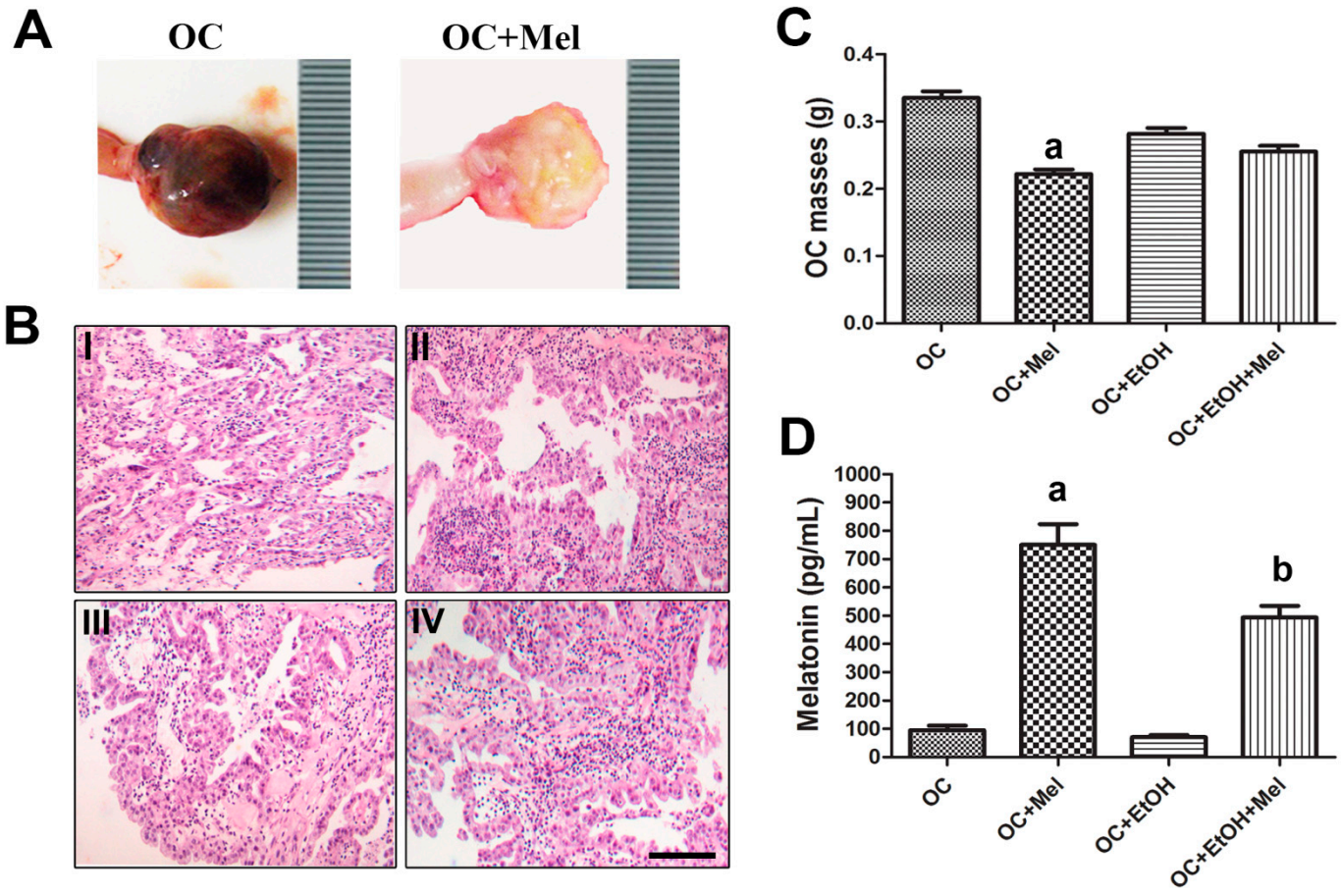

Figure 2

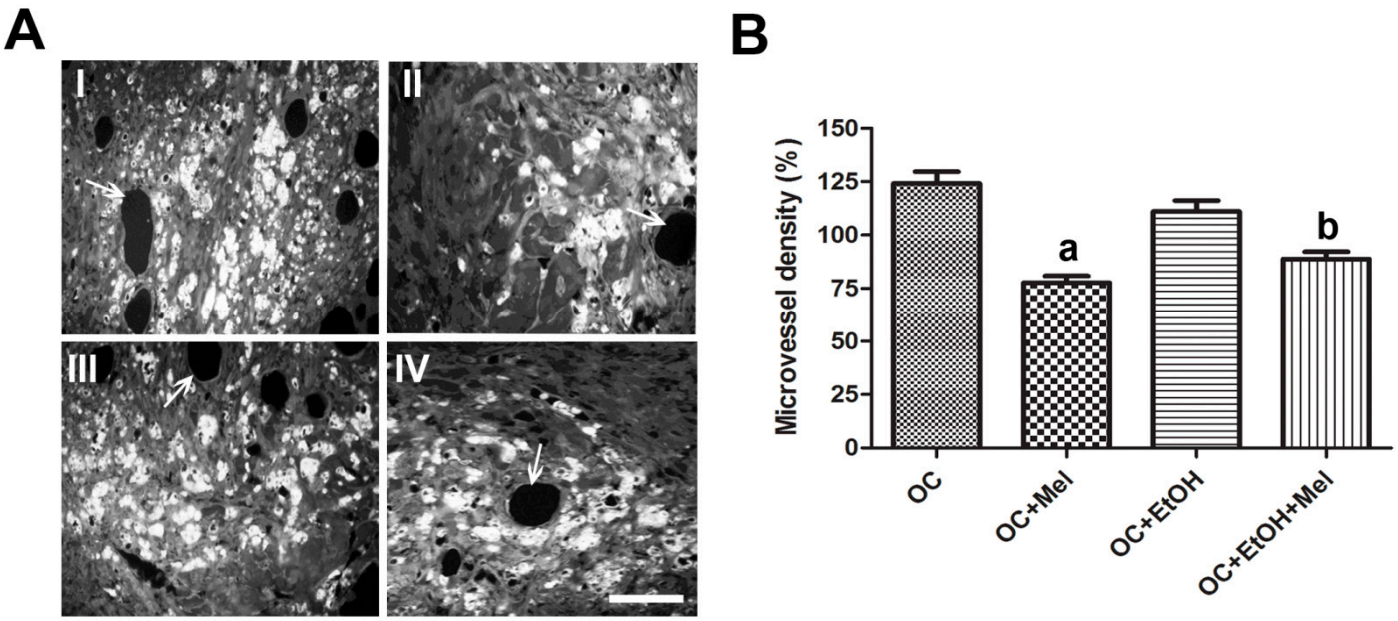

Figure 3

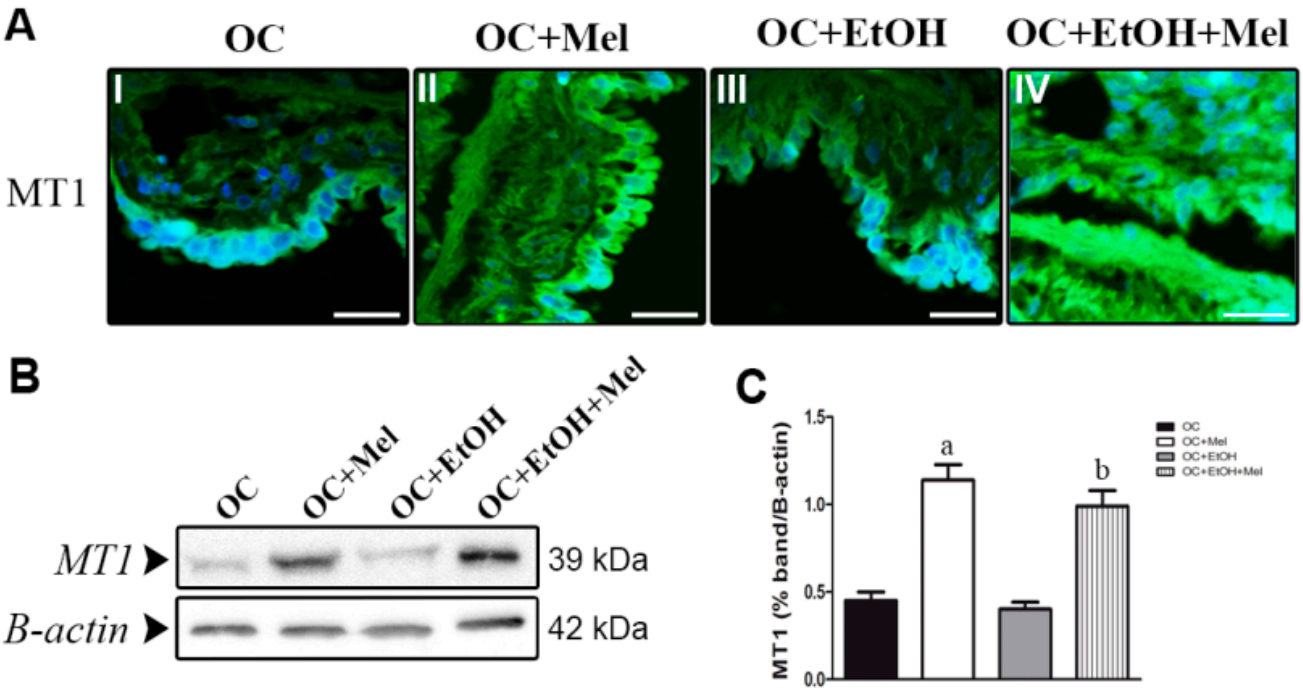

Preprints (www.preprints.org) | NOT PEER-REVIEWED | Posted: 6 March 2017 doi:10.20944/preprints201703.0026.v1

Peer-reviewed version available at Int. J. Mol. Sci. 2017, 18, , 763; doi:10.3390/ijms18040763

Figure 4

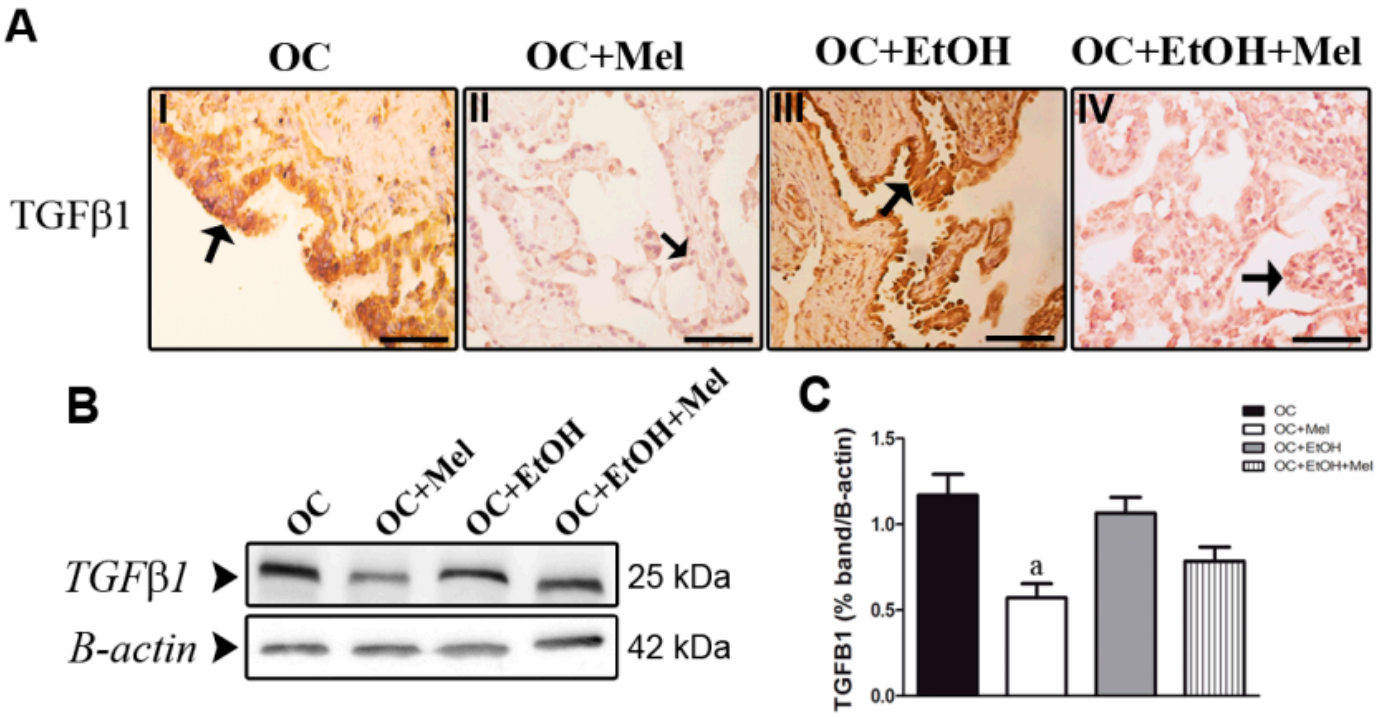

Figure 5

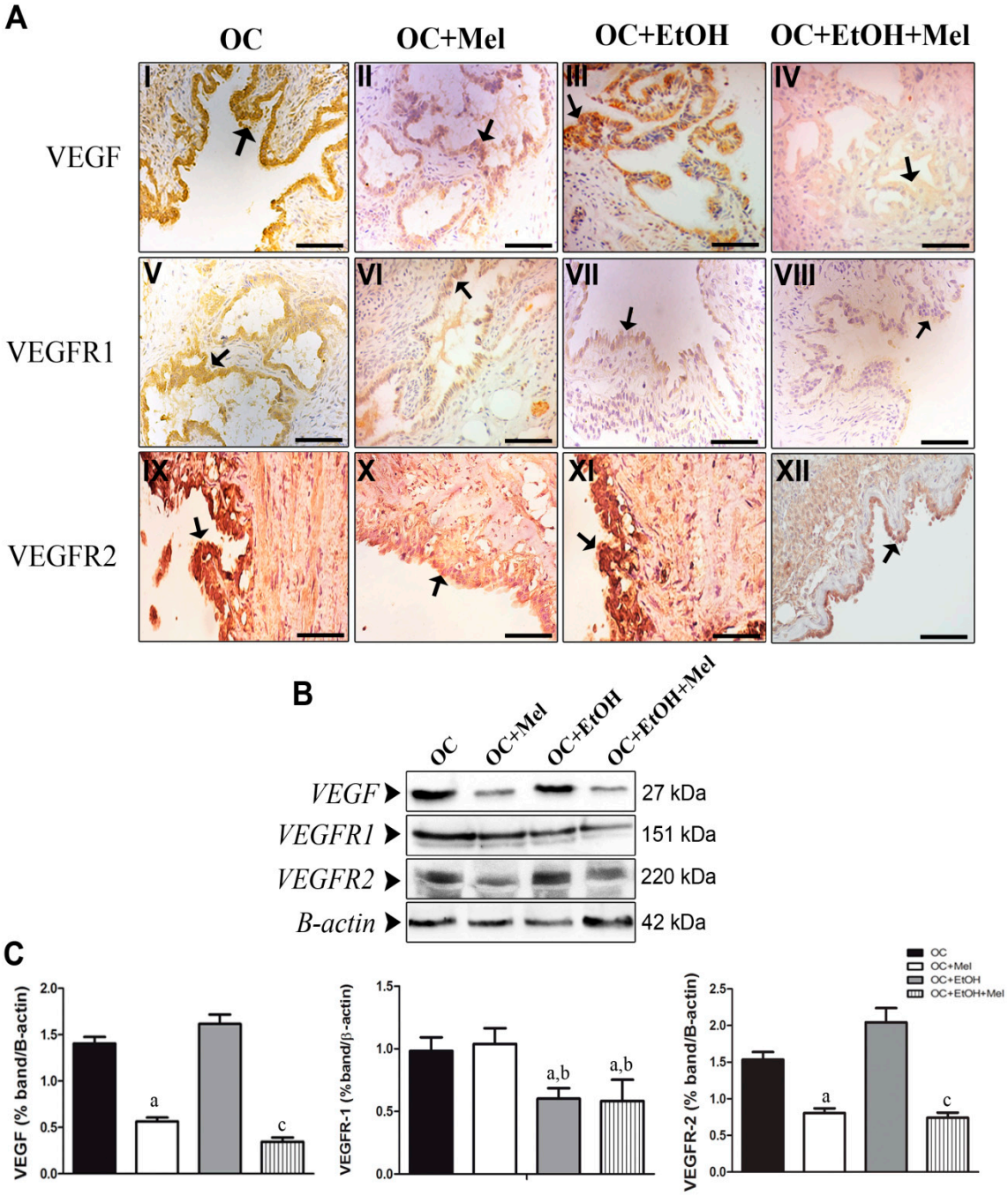

Figure 6

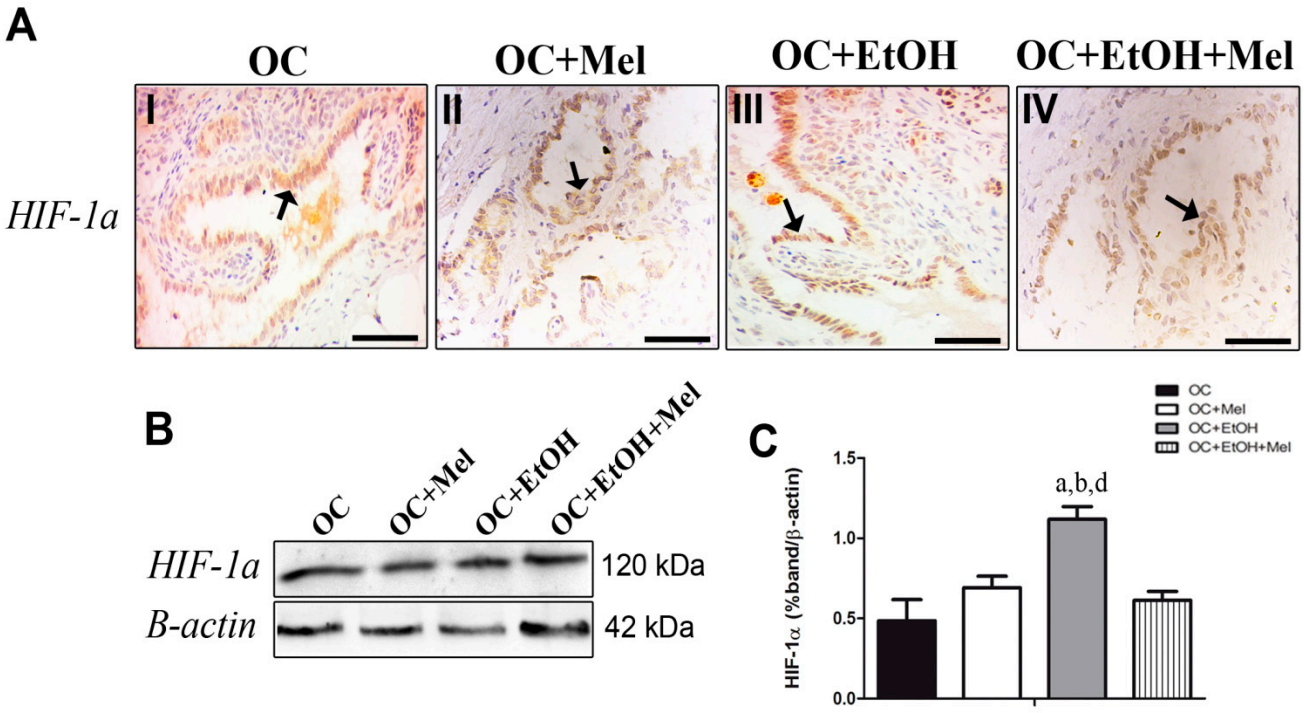

Peer-reviewed version available at Int. J. Mol. Sci. 2017, 18, , 763; doi:10.3390/ijms18040763

Figure 7